Supplemental Document

Biomedical Optics EXPRESS

Characterization of pathological stomach tissue using polarization-sensitive second harmonic generation microscopy: supplement

Hwanhee Jeon, MacAulay Harvey, Richard Cisek, Elisha Bennett, and Danielle Tokarz*

Department of Chemistry, Saint Mary's University, 923 Robie Street, Halifax, Nova Scotia, B3H 3C3, Canada
*danielle.tokarz@smu.ca

Supplement DOI: https://doi.org/10.6084/m9.figshare.24119316

Parent Article DOI: https://doi.org/10.1364/BOE.500335

Characterization of Pathological Stomach Tissue Using Polarization-sensitive Second Harmonic Generation Microscopy Supplement 1

HWANHEE JEON, MACAULAY HARVEY, ELISHA BENNETT, RICHARD CISEK, AND DANIELLE TOKARZ*

Department of Chemistry, Saint Mary's University, 923 Robie Street, Halifax, Nova Scotia, B3H 3C3, Canada
**danielle.tokarz@smu.ca*

Derivation of the Second-order Nonlinear Optical Susceptibility Tensors Assuming Trigonal (C_{3v}) and Kleinman Symmetries

The measured SHG ($I_{2\omega}$) intensity using the setup described can be determined using:

$$I_{2\omega} \propto |JE_{2\omega}|^2 \propto \left|J\,\chi^{(2)}{:}\,E_{\omega}{:}\,E_{\omega}\right|^2$$

where $E_{2\omega}$ is the second harmonic field, E_{ω} is the fundamental electric field, $\chi^{(2)}$ is the second-order electric susceptibility, and J is the Jones matrix of the analyzer given by

$$J = \begin{pmatrix} \sin^2\phi & sin\phi cos\phi \\ sin\phi cos\phi & \cos^2\phi \end{pmatrix}$$

For a structure having C_{3V} symmetry about the Z axis the $\chi^{(2)}$ tensor contains only four independent nonzero elements $\chi^{(2)}_{ZZZ}$, $\chi^{(2)}_{XXZ} = \chi^{(2)}_{XZX} = \chi^{(2)}_{YZY} = \chi^{(2)}_{YYZ}$, $\chi^{(2)}_{ZXX} = \chi^{(2)}_{ZYY}$, $\chi^{(2)}_{XXX} = -\chi^{(2)}_{XYY} = -\chi^{(2)}_{YYX} = -\chi^{(2)}_{YXY}$. Now using $E_{\omega} \propto \begin{pmatrix} sin\theta \\ cos\theta \end{pmatrix}$ we obtain the following.

$$I_{2\omega} \propto \left|\frac{\chi^{(2)}_{ZZZ}}{\chi^{(2)}_{ZXX}}\cos^2\theta\, cos\phi + \frac{\chi^{(2)}_{XXX}}{\chi^{(2)}_{ZXX}}\sin^2\theta\, sin\phi + \frac{\chi^{(2)}_{XXZ}}{\chi^{(2)}_{ZXX}} sin2\theta sin\phi + \sin^2\theta\, cos\phi\right|^2$$

where $\chi^{(2)}_{ZZZ}/\chi^{(2)}_{ZXX}$ is expressed as ρ and $\chi^{(2)}_{XXX}/\chi^{(2)}_{ZXX}$ is expressed as S. We additionally assume that $\chi^{(2)}_{XXZ} = \chi^{(2)}_{ZXX}$, similar to previous researchers [1].

References

1. R. Ambekar, T.-Y. Lau, M. Walsh, R. Bhargava, and K. C. Toussaint, "Quantifying collagen structure in breast biopsies using second-harmonic generation imaging," Biomed Opt Express 3, 2021–2035 (2012).

Larger View of PIPO SHG Analysis of Normal Gastric Tissue Demonstrating ρ and S

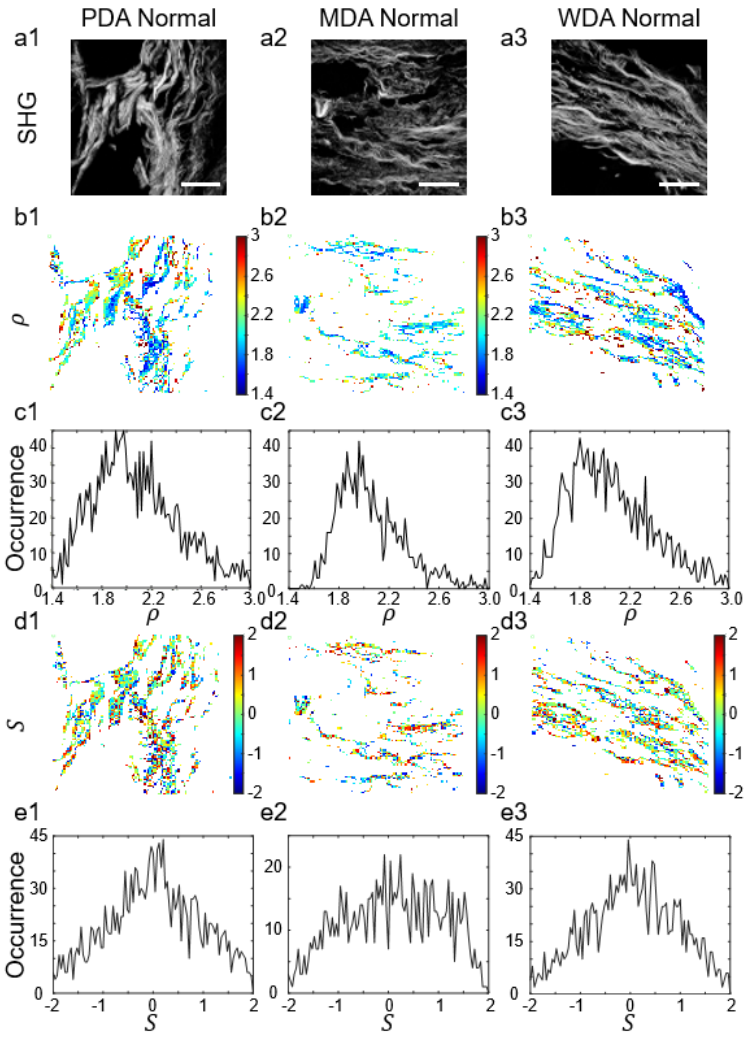

Fig. S1. Enlarged Figure 2a-e for 1-3 from the paper. The scale bar in a1-a3 represents 25 μm.

PIPO SHG Analysis of Cancerous Gastric Tissue Demonstrating ρ and S

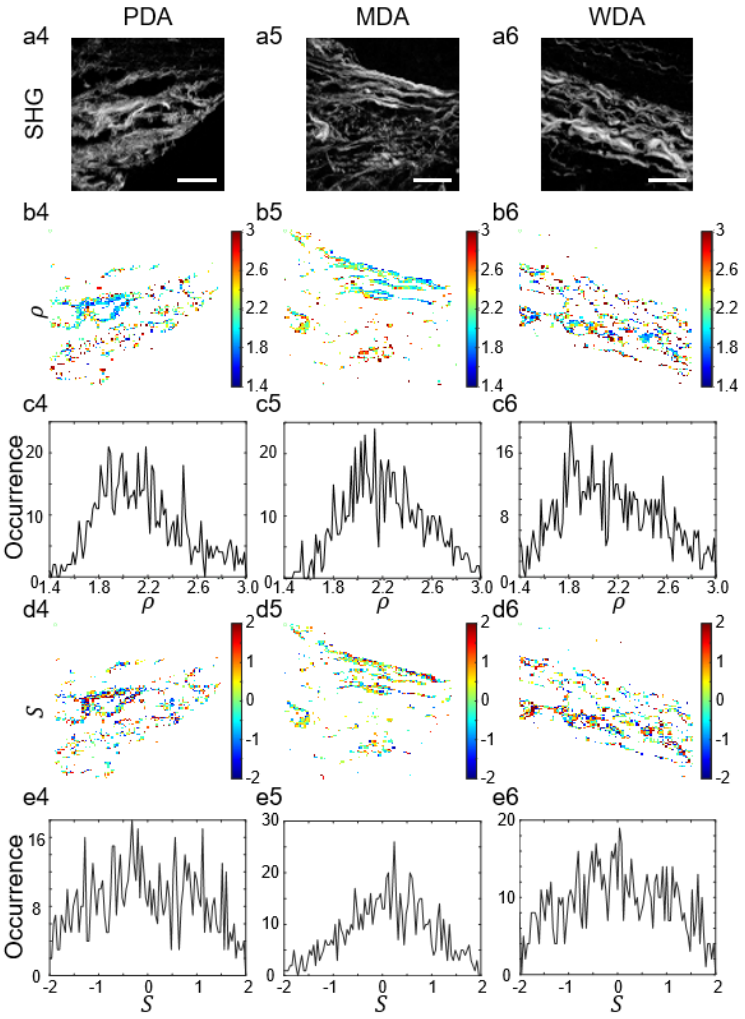

Fig. S2. Enlarged Figure 2a-e for 4-6 from the paper. The scale bar in a4-a6 represents 25 μm.

PIPO SHG Analysis of Gastric Tissue Demonstrating κ and DOLP

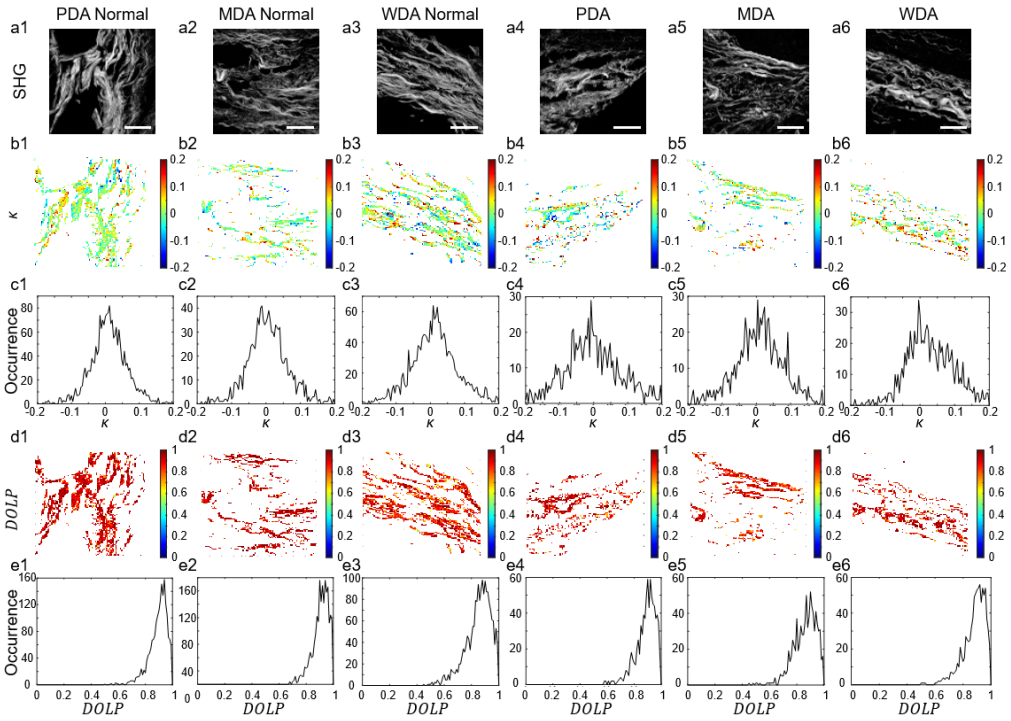

Fig. S3. PIPO SHG analysis of gastric tissue in patients diagnosed with adenocarcinoma. Normal gastric tissue from patients who were diagnosed with poorly differentiated adenocarcinoma (PDA, a1-e1), moderately differentiated adenocarcinoma (MDA, a2-e2) and well differentiated adenocarcinoma (WDA, a3-e3) as well as tumor tissue diagnosed as PDA (a4-e4), MDA (a5-e5) and WDA (a6-e6) from the same patients. A simple summation of 65 SHG logarithmic intensity images (a1-a6). Color-coded maps of the fitted κ values (b1 – b6) and occurrence frequency histograms of the κ values (c1 – c6). Color-coded maps of DOLP values for fitted pixels (d1 – d6) and occurrence frequency histograms of the DOLP values (e1 – e6). The scale bar in a1-a6 represents 25 µm.

Larger View of PIPO SHG Analysis of Normal Gastric Tissue Demonstrating κ and DOLP

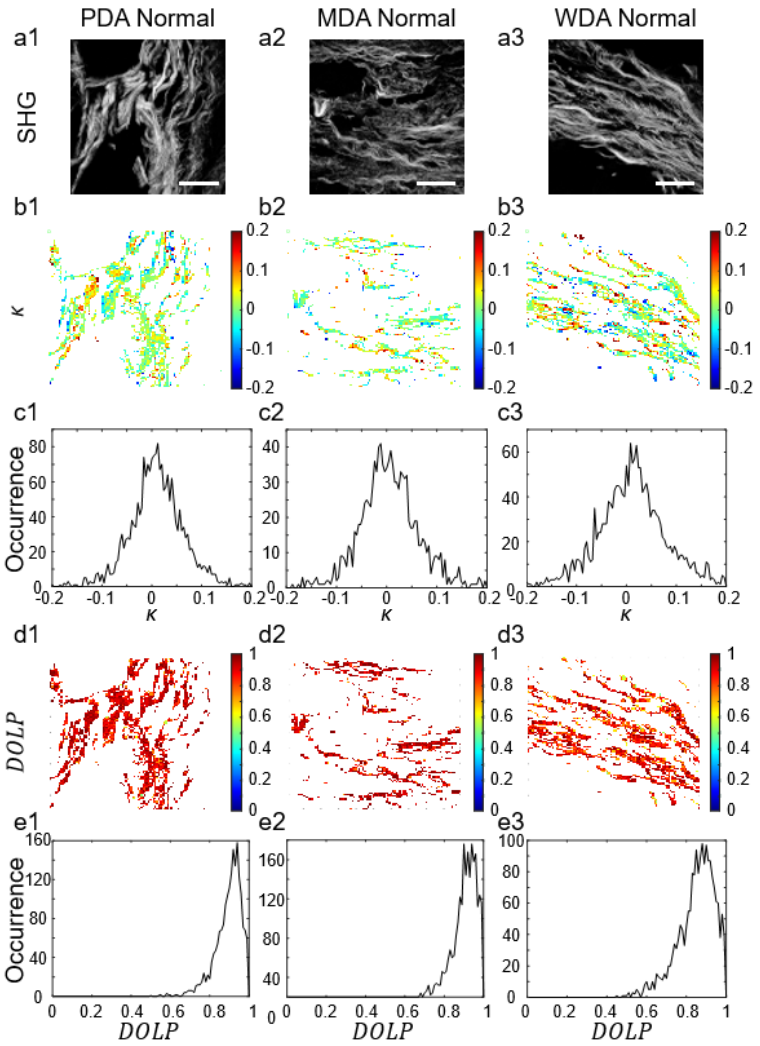

Fig. S4. Enlarged Figure S4a-e for 1-3. The scale bar in a1-a3 represents 25 μm.

Larger View of PIPO SHG Analysis of Cancerous Gastric Tissue Demonstrating κ and DOLP

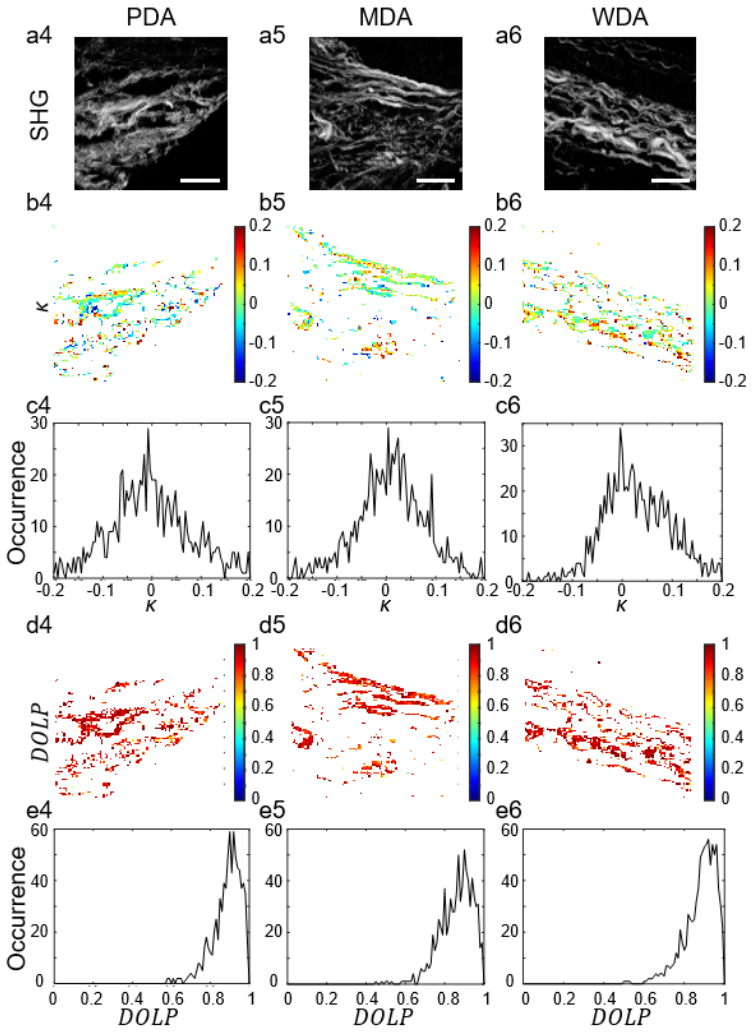

Fig. S5. Enlarged Figure S4a-e for 4-6. The scale bar in a4-a6 represents 25 μm.

Numerical Simulations of ρ and $|S|$ versus the Angle Between Two Intersecting Cylindrically Symmetric Structures with Identical Diameters

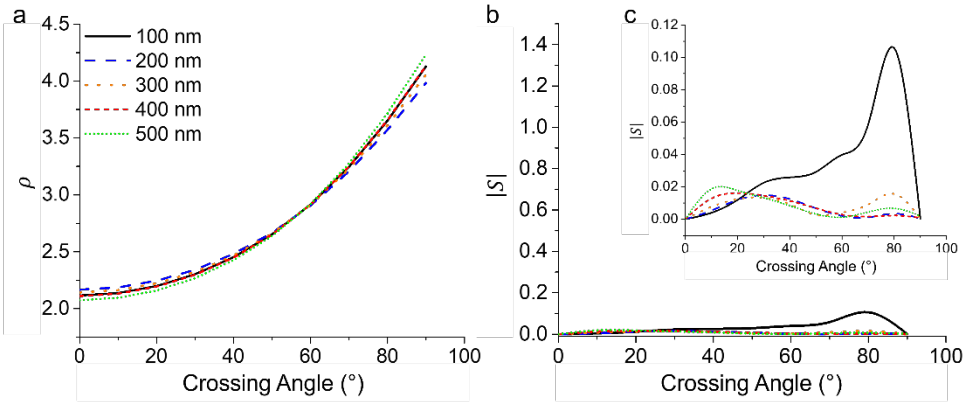

Fig. S6. Numerically simulated PIPO SHG datasets fitted with Eq. 2, revealing ρ (a) and $|S|$ (b, c) values of intersecting cylindrically symmetric structures versus the angle between the two structures. Graphs a, b and c depict two cylindrically symmetric structures with the same diameter as a function of crossing angle, with diameters ranging between 100 and 500 nm. Note that the inset graph labeled c is the same graph as b with zoomed-in y-axes to show the oscillation in $|S|$.

Numerical Simulations of ρ and $|S|$ versus the Angle Between Two Intersecting Cylindrically Symmetric Structures with Differing Diameters

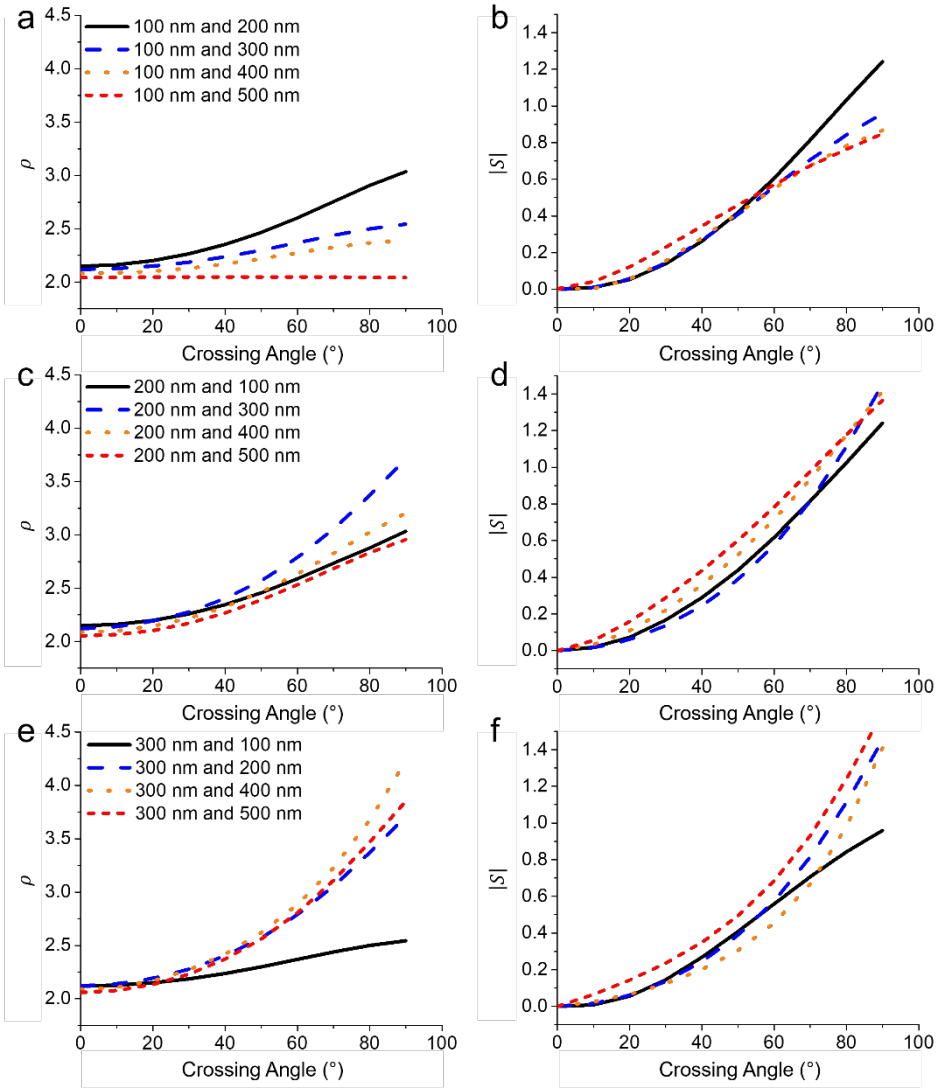

Fig. S7. Numerically simulated PIPO SHG datasets fitted with Eq. 2, revealing ρ (a, c, e) and corresponding $|S|$ (b, d, f) values of intersecting cylindrically symmetric structures versus the angle between the two structures. Graphs depict two cylindrically symmetric structures with different diameters as a function of crossing angle, with diameters ranging between 100 and 500 nm.

Data Set 1: Polarization-in, Polarization-out (PIPO) SHG Data for Cancerous and Normal Tissues

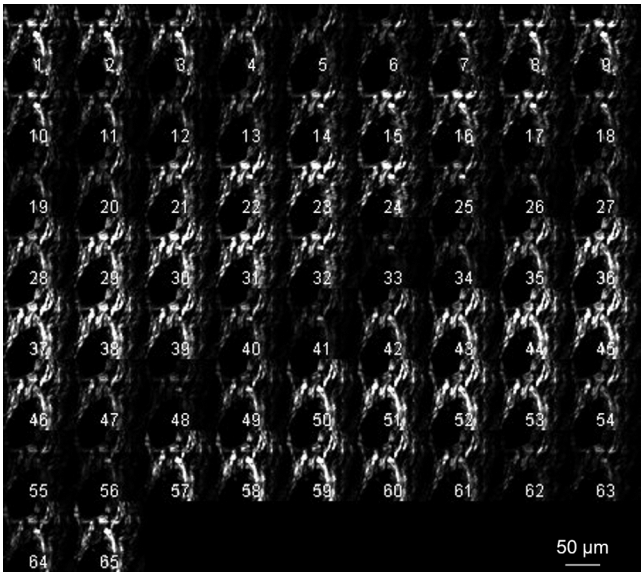

Fig. S8. A montage of PIPO SHG images of PDA normal (Fig. 1a1 in the paper). In total, 65 are collected at varying polarizer and analyzer angles.

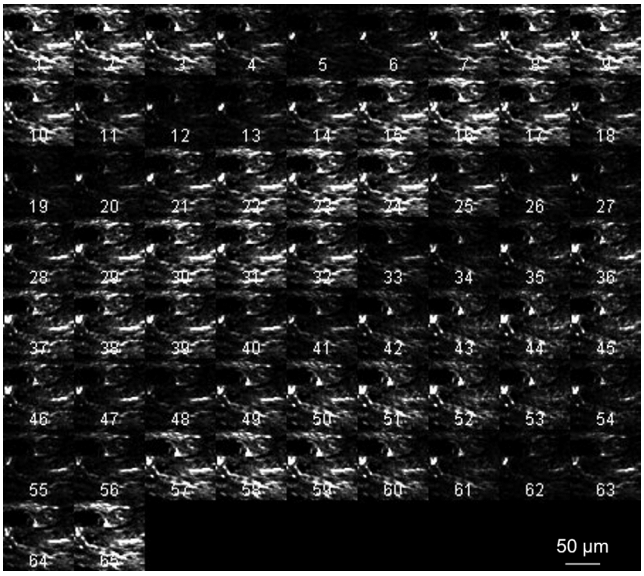

Fig. S9. A montage of PIPO SHG images of MDA normal (Fig. 1a2 in the paper). In total, 65 are collected at varying polarizer and analyzer angles.

Fig. S10. A montage of PIPO SHG images of WDA normal (Fig. 1a3 in the paper). In total, 65 are collected at varying polarizer and analyzer angles.

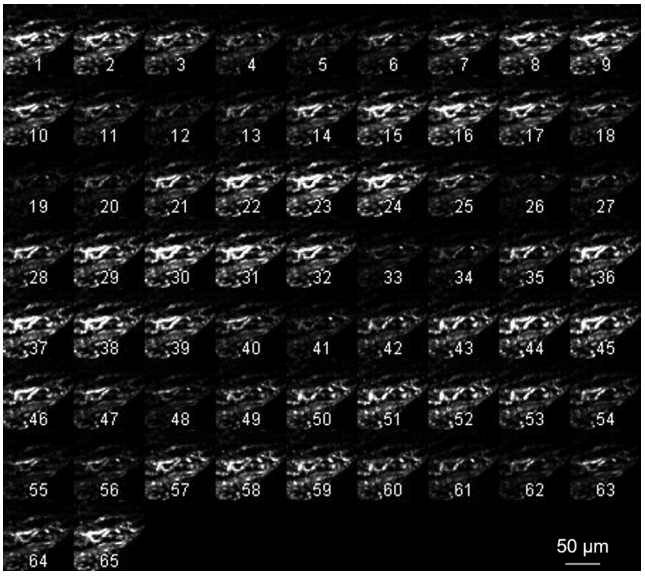

Fig. S11. A montage of PIPO SHG images of PDA (Fig. 1a4 in the paper). In total, 65 are collected at varying polarizer and analyzer angles.

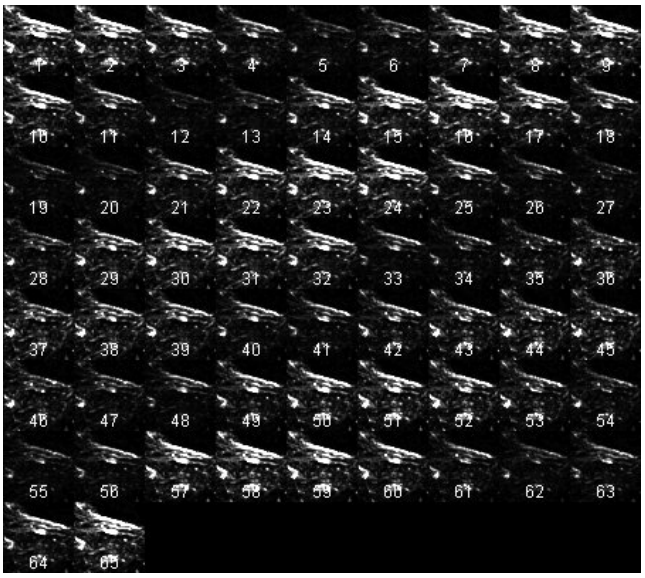

Fig. S12. A montage of PIPO SHG images of MDA (Fig. 1a5 in the paper). In total, 65 are collected at varying polarizer and analyzer angles.

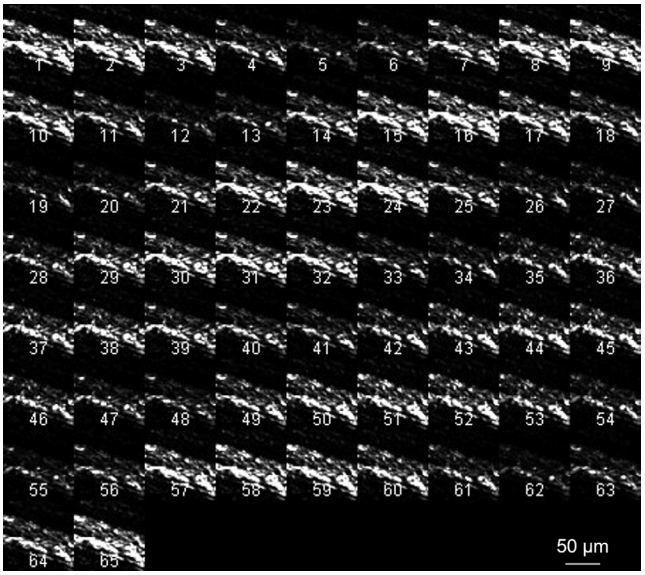

Fig. S13. A montage of PIPO SHG images of WDA (Fig. 1a6 in the paper). In total, 65 are collected at varying polarizer and analyzer angles.